Talanta 204 (2019) 395–401

Contents lists available at ScienceDirect

Talanta

journal homepage: www.elsevier.com/locate/talanta

Label-free nanostructured biosensor for *Schistosoma mansoni* detection in complex biological fluids

Giselle S. Santos[a,b], Raquel G.S.C. Caldas[b], Fabio L. Melo[c], Igor S. Bruscky[d], Maria A.L. Silva[c], Leandro B. Wanderley[e], Cesar A.S. Andrade[b], Maria D.L. Oliveira[a,b,*]

[a] Programa de Pós-Graduação em Bioquímica e Fisiologia, Universidade Federal de Pernambuco, 50670-901 Recife, PE, Brazil
[b] Departamento de Bioquímica, Universidade Federal de Pernambuco, 50670-901 Recife, PE, Brazil
[c] Departamento de Parasitologia, Instituto Aggeu Magalhaes /FIOCRUZ, 50670-420, Recife, PE, Brazil
[d] Faculdade de Medicina, UNINASSAU, 51021-140, Recife, PE, Brazil
[e] Centro Universitário Brasileiro – UNIBRA, 50050-230, Recife, PE, Brazil

ARTICLE INFO

Keywords:
Schistosoma mansoni
Genosensor
Nanoparticles
Electrodeposition
Electrochemical impedance spectroscopy
Cyclic voltammetry

ABSTRACT

Schistosomiasis is a neglected tropical disease with a worldwide prevalence. Neuroschistosomiasis is the most severe presentation of the disease and affects the central nervous system. In this work, *Schistosoma mansoni* detection was based on self-assembled layers of 3-mercaptopropyltrimethoxysilane (MPTS) and electrosynthesized gold nanoparticles (AuNPs). The DNA probe was chemisorbed onto AuNPs. The biosensor was characterized by electrochemical impedance spectroscopy (EIS) and cyclic voltammetry (CV). The impedimetric response of the MPTS-AuNPs-DNA_{probe} system indicates an effective modification of the electrode surface. Topographical atomic force microscopy images were used to characterize the self-assembled layers on the gold electrode surface. The proposed biosystem was able to recognize the *S. mansoni* genome sequence at different concentrations in samples of urine, cerebrospinal fluid, and serum. Several concentration ranges were evaluated: urine (27–50 pg μL^{-1}), cerebrospinal fluid (25–60 pg μL^{-1}), and serum (27–42 pg μL^{-1}). The limit detection (LOD) of the biosensor was 0.6 pg μL^{-1}. The developed label-free genosensor was able to detect small concentrations of *S. mansoni* DNA in complex biological fluids.

1. Introduction

Schistosomiasis has a critical role for public health with socioeconomic impacts on impoverished communities [1]. Of note, chronic S. mansoni infection leads to significant residual morbidity. The disease remains a devastating neglected tropical disease that affects approximately 260 million people worldwide [2,3]. Also, about 800 million people are currently at risk of developing schistosomiasis worldwide [4,5].

The symptomatology of the acute phase is related to fever, diarrhea, headache, asthenia, and anorexia, or even asymptomatic [6]. The continuous infections can result in granulomatous reactions and fibrosis in the affected organs. Also, these manifestations can occur associated with lesions of the central nervous system, polyposis with bloody diarrhea, splenomegaly, portal hypertension, and pulmonary hypertension [7]. Neuroschistosomiasis (NS) can clinically manifest as meningomyeloradiculitis, myelitis, and radiculitis. In addition, cerebral, pseudotumoral, or spinal forms are also observed. Medullary schistosomiasis is the most severe clinical manifestation of the S. mansoni infection [8].

The intestinal schistosomiasis diagnosis is usually performed through the Kato-Katz fecal smear technique (a standard method recommended by the World Health Organization for qualitative and quantitative determination). However, the Kato-Katz technique is limited due to its low sensitivity, particularly in mild infections [9,10]. Immunological assays are used for performing the routine laboratory tests, especially in the chronic-phase chagasic infection [11]. The immunological assays are intradermal reaction, complement fixation reaction, indirect immunofluorescence, enzyme-linked immunosorbent assay (ELISA), and capture ELISA [12]. In addition, the immunological assays are dependent on the search for S. mansoni antibodies [13,14].

However, antibodies-based tests present limitations due to the cross-reaction with other antigens (mainly of other helminths), difficulty of differentiating from the active infection of the previous contact with the parasite, and low sensitivity for asymptomatic cases [15]. Cerebrospinal fluid (CSF) is extensively used for diagnosis of patients with

* Corresponding author. Departamento de Bioquímica, UFPE, 50670-901, Recife, PE, Brazil.
E-mail address: m_danielly@yahoo.com.br (M.D.L. Oliveira).

https://doi.org/10.1016/j.talanta.2019.05.111
Received 12 March 2019; Received in revised form 29 May 2019; Accepted 29 May 2019
Available online 31 May 2019
0039-9140/

clinically suspected NS [16].

In this context, electrochemical genosensors have become an alternative for the development of new diagnostic methods [17,18]. Nanomaterials have been used for the development of biodevices due to their huge surface-to-volume ratio, controlled size, and differentiated physicochemical properties. In addition, nanomaterials are extensively used to immobilize the recognition elements (e.g., DNA or proteins) [19].

AuNPs are the most commonly used nanomaterial in biosensor development through biomolecules conjugation [19]. AuNPs have been used associated with different nanomaterials as graphene oxide (GO) and carbon nanotubes (CNT) to obtain hybrids nanoplatforms for DNA detection [19,20]. Hybrids nanoplatforms improve the sensor performance due to the large surface area and good electrical conductivity attributed to a synergistic effect of these nanomaterials [21–24]. Electrochemical techniques can monitor variations in the electrical properties (resistance or capacitance) of the electrode surface [25]. Potentiodynamic methods (e.g., potential cycling) are suitable for obtaining AuNPs on the electrode surface [26,27]. Thus, impedimetric nanosensors are potentially promising due to their potential for rapid DNA detection with low cost and sensitivity [25,28].

In this connection, the present study evaluated the assembly process of the 3-mercaptopropyltrimethoxysilane (MPTS) and electrochemically synthesized AuNPs (Fig. 1) for S. mansoni genome detection. The organosilane (MPTS) was used to obtain compelling sol-gel derivative films to immobilize AuNPs since it interacts with the working electrode through Au–S bonds [29]. AuNPs were electrochemically synthesized, and the applied potential cycling controls the nucleation/growth process of the AuNPs [30]. Also, AuNPs offer a unique approach for immobilization of thiol-modified DNA. Therefore, the association of sol-gel derivative films with AuNPs allows the development of a genosensor for S. mansoni detection in CSF and other biological fluids.

2. Materials and methods

2.1. Materials

DNA samples of *S. mansoni* were assigned by the Department of Parasitology of the Aggeu Magalhães Institute (Recife, Brazil). RT-qPCR was useful for the previous characterization of all samples. 3-Mercaptopropyltrimethoxysilane (MPTS), Gold chloride (III) hydrate ($HAuCl_4 \cdot xH_2O$), and bovine serum albumin (BSA) were purchased from Sigma-Aldrich (St. Louis, MO, USA). Ferrocyanide and potassium ferrocyanide were obtained from VETEC (Brazil). DNA solutions were prepared in phosphate-buffered saline (PBS, pH 7.4). The other chemicals used in this work were reagent grade and used as received without further purification. Ultrapure water was obtained from a Millipore Milli-Q system.

2.2. Sample preparation

Controls and patient's samples were collected (v = 1 mL) and their analyses consisted of general and specific cell counts, glucose, CSF, protein electrophoresis, and immunological determinations (ELISA) for schistosomiasis, herpes, syphilis, cysticercosis, toxoplasmosis, cytomegalovirus, Epstein-Barr virus, human immunodeficiency virus, varicella zoster, Cryptococcus, and human cell lymphotropic virus. The samples were also analyzed by nPCR [8]. Electrophoresis using genomic DNA from *S. mansoni* at different concentrations is shown in Fig. S1.

The urine samples (v = 5 mL) were transferred to a 15-mL Falcon tube. DNA was extracted according to Silva using protocol 2 [31]. Schistosome DNA was purified using the illustrated tissue & cells genomic Prep Mini Spin Kit (GE Healthcare, UK) according to the manufacturer's instructions. DNA samples from patients were extracted and purified using the illustrated blood genomic Prep Mini Spin Kit (GE Healthcare, UK) according to the manufacturer's instructions. Thus, it was quantified in a spectrophotometer and stored at −20 °C. The thiolated specific primer for *S. mansoni* was Schfo17 (5′-GTGCTGGT GGGTTGACGAGTTC-3′) [32].

2.3. Modification of the electrode surface

Initially, 50 mM MPTS solution was prepared by mixing MPTS with deionized water (0.5:100, v/v) and 600 µL of 0.1 mol L^{-1} HCl [33]. Then, the mixture was sonicated for 9 min followed by stirring for 45 min until obtaining a transparent homogeneous solution. The electrode surface was gently polished with sandpaper and deionized water. Subsequently, the bare gold electrode (BGE) was immersed in a solution of sodium hypochlorite for 10 min, washed with deionized water, and dried at room temperature. After, the electrode surface was modified with 4 µL of the homogeneous solution of MPTS by drop coating and allowed to dry at 25 °C. Subsequently, 1 mM de $HAuCl_4 \cdot xH_2O$ in

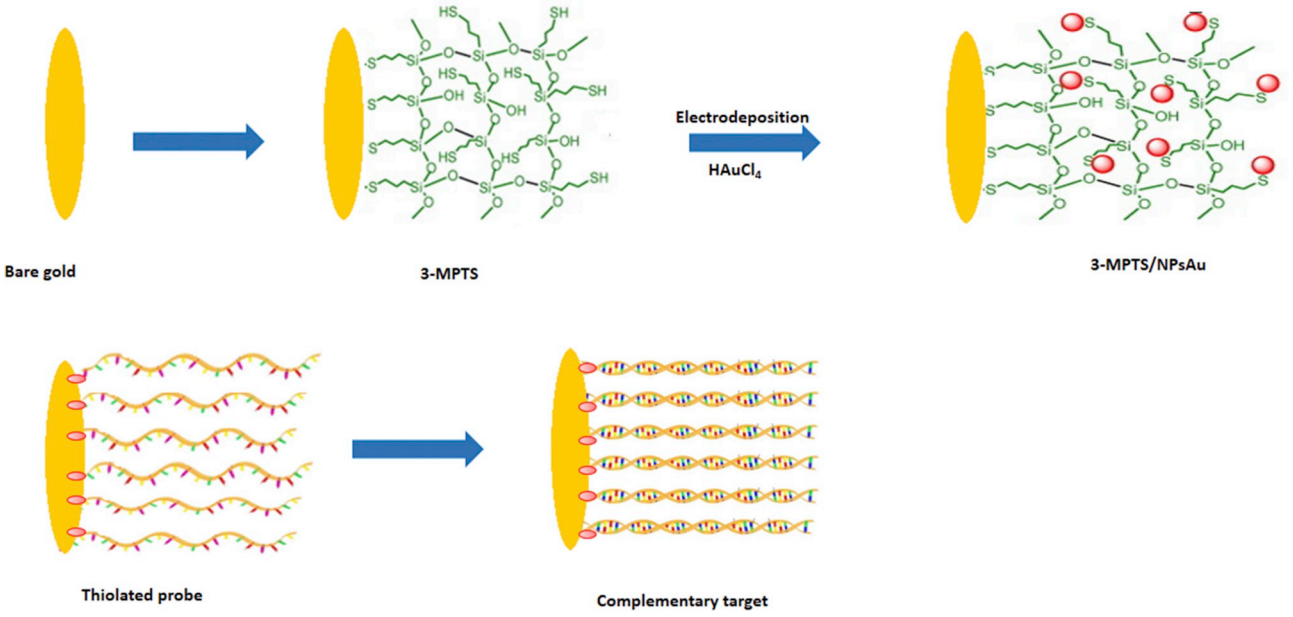

Fig. 1. Schematic representation of the fabrication process of the biosensor.

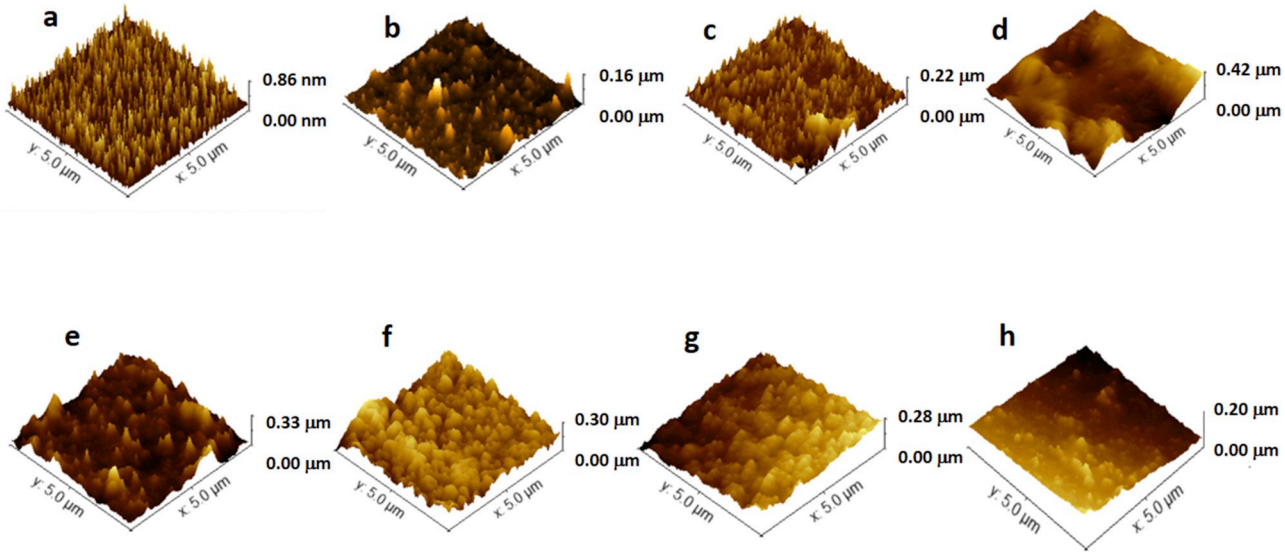

Fig. 2. AFM images for the stepwise modification process: **a)** MPTS_AuNPs; **b)** MPTS_ AuNPs-$DNA_{probe;}$ **c)** MPTS_ AuNPs-DNA_{probe}-DNA_{worm}; **d)** MPTS_ AuNPs-DNA_{probe}-$DNA_{Serum\ Sample}$ **e)** MPTS_ AuNPs-DNA_{probe}-$DNA_{Urine\ sample}$; **f)** MPTS_ AuNPs-DNA_{probe}-$DNA_{CSF\ sample}$; **g)** MPTS_ AuNPs-$DNA_{probe\text{-}negative\ control}$.

0.5 mol L^{-1} H_2SO_4 was cycled 30 times in the range of potentials between +1.3 V and −0.2 V at a scan rate of 50 mV s^{-1}. AuNPs were directly deposited on the working electrode previously modified with MPTS. BSA was used in all experiments to avoid non-specific interactions.

2.4. Hybridization analysis

Target DNA was diluted in 10 mM PBS solution (pH 7.4), heated for 3 min at 40 °C (to denature the double-stranded DNA into single strands), and followed by hybridization with a complementary probe. Hybridization was performed by a simple drop-coating method using 2 µL of the target DNA obtained from CSF, urine, and serum at different concentrations. We also evaluated the electrochemical response of the biosensor after exposure to DNA samples containing ascorbic acid and cholesterol as interferents. In these assays, 2 µL of each sample was dropped on the sensor surface for 15 min. The selectivity study was carried out in 10 mM PBS solution (pH 7.4) containing 2 µL of the analyte and of each interferent. The stability was analyzed through the sensor responses after immersion in 5 mM NaOH solution and subsequent immobilization of the target DNA.

2.5. Electrochemical measurements

Cyclic voltammetry and electrochemical impedance measurements were performed using a PGSTAT 128N potentiostat/galvanostat (Autolab, The Netherlands) at room temperature. A three-electrode configuration was employed with an Ag/AgCl reference electrode (saturated KCl), a platinum wire electrode as the auxiliary electrode, and the gold electrode (BGE) as the working electrode. The impedance spectra were recorded within the 100 mHz and 100 kHz frequency range with an alternating voltage adjusted to an amplitude of 10 mV. The CV analysis was performed in the potential range between +0.7 V and −0.2 V at a scan rate of 50 mV s^{-1}. The electrolytic solution was 10 mM $K_4[Fe(CN)_6]^{4-}$/$K_3[Fe(CN)_6]^{3-}$ (1:1, v/v) in 20 mM PBS (pH 7.4). All electrochemical measurements were performed in triplicate (n = 3).

2.6. Atomic force microscopy measurements

AFM was used to perform structural analyses of the system in a non-contact mode in the air at room temperature (t = 25 °C) [34]. Cantilevers with an AFM silicon probe (Nanoworld, Japan, resonance frequency = 300 kHz, spring constant = 42 Nm-^{1}) were used for all measurements. The images were collected with a scanning rate of 1.0 Hz in a scan area of 5 × 5 µm. The images were obtained from at least two macroscopically separated areas. The Gwyddion software was used to analyze the AFM images [35].

3. Results and discussion

3.1. Morphological characterization

Fig. 2a and b shows the BGE surface after modification with MPTS and electrodeposited AuNPs, respectively. Then, surfaces with a roughness of 0.86 nm (Figs. 2a) and 0.16 µm (Fig. 2b) were obtained, suggesting an efficient assembly of the layers. MPTS provides a 3D polymeric network with thiol tail groups that binds to gold surfaces. Also, this matrix provides a biocompatible environment that preserves the biological structure and activity after immobilization process. The polymeric network is essential to AuNPs assembly allowing the incorporation of a high amount of biomolecules that improve the sensor sensitivity. DNA probe immobilization resulted in changes of the surface roughness to 0.22 µm (Fig. 2c) in agreement with previous studies reported in the literature [33,36].

The specific interaction of the sensor and *S. mansoni* samples was evaluated. Significant changes in topography were observed for worm DNA (Fig. 2d), contaminated serum samples (Fig. 2e), urine (Fig. 2f), and LCR (Fig. 2g). The non-complementary target shows a homogeneous distribution on the electrode surface without the presence of aggregates (Fig. 2h). Thus, our results confirm the specificity of the sensor. AFM imaging is in good agreement with CV and EIS results.

3.2. Electrochemical characterization

The electrochemical characterization of the modified electrode was performed through cyclic voltammetry and electrochemical impedance spectroscopy. From Fig. 3a, we can observe a decrease in the anodic peak current after the addition of MPTS (curve b) as compared to the unmodified electrode (curve a). Thus, we obtained an effective assembly of the MPTS layer on the electrode surface. The decreased current can be attributed to the increased steric hindrance of MPTS [37]. An increase of the anodic and cathodic peak currents was verified due to AuNPs electrodeposition, which results in a rise in the surface area and improvement of the conductivity (curve c). Further wane in

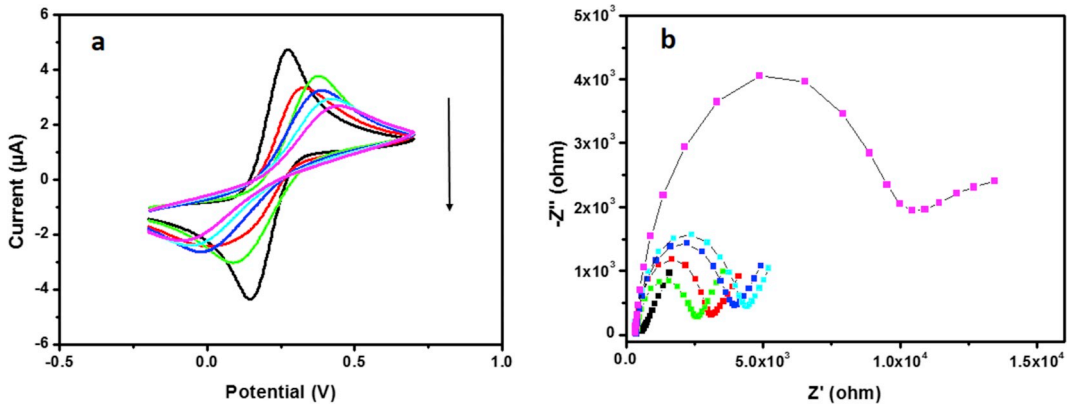

Fig. 3. (a) Cyclic voltammograms of the steps of electrode modification and bio-recognition processes: BGE (), MPTS, MPTS_AuNPs, MPTS_ AuNPs-DNA_{probe}, MPTS_AuNPs-DNA_{probe}-BSA, MPTS_ AuNPs-DNA_{probe}-genome. Cyclic voltammetry scan was initiated at - 0.2 V vs. Ag/AgCl in positive direction at 50 mV s^{-1}. **(b)** Nyquist plots for the stepwise modification process: BGE (•), MPTS ●, MPTS_AuNPs ●, MPTS_AuNPs-DNA_{probe} ●, MPTS_AuNPs-DNA_{probe}-BSA ●, MPTS_AuNPs-DNA_{probe}-genome ●.

the currents is observed after immobilization of the thiol-modified DNA probe on the MPTS-AuNPs system (curve d). BSA was used to block the remaining sites (curve e). In particular, after the hybridization process with the complementary genome, a further decrease in the anodic and cathodic peaks (curve f) was obtained due to additional blockage of the electron transfer to the electrode surface. Fig. 3b shows the impedance spectra of each stage of the sensor platform development in a frequency range between 100 mHz and 100 kHz. Significant differences in the impedance spectra were observed during the assembly of the sensor platform when compared to the unmodified gold electrode since each layer acts as a mass transfer block layer [34,38].

The electrochemical response of the genosensor was evaluated after exposure to different concentrations of target DNA (0.6, 1.3, 2.6, 5.2, 10.4, 20.9, 40.0, and 83.9 pg μL^{-1}). A nonconductive complex formation occurs after the recognition of the contaminated samples that difficult the passage of the faradaic current to the transducer [40]. The voltammetric response of the genosensor is proportional to the number of recognized molecules (Fig. 4a).

A modified Randles equivalent circuit was used [41] to fit the impedance data (Fig. 4b, solid lines). We obtained a good agreement between the equivalent circuit model and the experimental results. The circuit is composed of resistance of the solution (Rsol), charge transfer resistance (Rct), constant phase element (CPE), and Warburg diffusion element (W). Ideally, W and Rsol represent the mass properties and diffusion characteristics of the redox probe in solution, respectively. CPE represents a non-ideal characteristic of double layer capacitance [42].

The performance of the genosensor was evaluated by the relative variation of R_{CT} (ΔR_{CT}), providing quantitative information of the DNA hybridization processes. The ΔR_{CT} was calculated according to the following equation:

$$\Delta R_{CT}\,(\%) = ([(R_{CT(recog)} - R_{CT(sensor)}]/R_{CT(sensor)})\times 100,$$

where $R_{CT(recog)}$ is the value of the electron transfer resistance of the sensor system after the biorecognition process, and $R_{CT(sensor)}$ is the value of the charge transfer resistance of the genosensor. The R_{CT} element depends on the insulating characteristic at the electrode/electrolyte interface. The filling of the recognition sites (Θ) was calculated using the following equation $\Theta = (1\text{-}R_S)/R_H$, where R_S is the R_{CT} of the biosensor and R_H is the R_{CT} of the biosensor after exposure to different concentrations of the genomic target sequence. Θ as a function of the concentration of the genomic target sequence is shown in Fig. 5. The value increases with increasing target DNA concentration and is found in 0.74 (74%) at a concentration of 83.9 pg μL^{-1}.

A linear behavior was obtained from 0.6 to 10.4 pg μL^{-1} (inset of Fig. 5b). However, after this range of concentrations, a saturation profile is observed. The changes in R_{CT} are higher than those of other impedance components. Thus, R_{CT} was used to evaluate the interfacial properties of the sensor system.

3.3. Detection of S. mansoni in different biological fluids (cerebrospinal fluid, urine, and serum)

CSF is an important laboratory sample for diagnosis in patients with suspected neuroschistosomiasis [13]. Therefore, we performed electrochemical analysis of CSF samples from patients diagnosed with

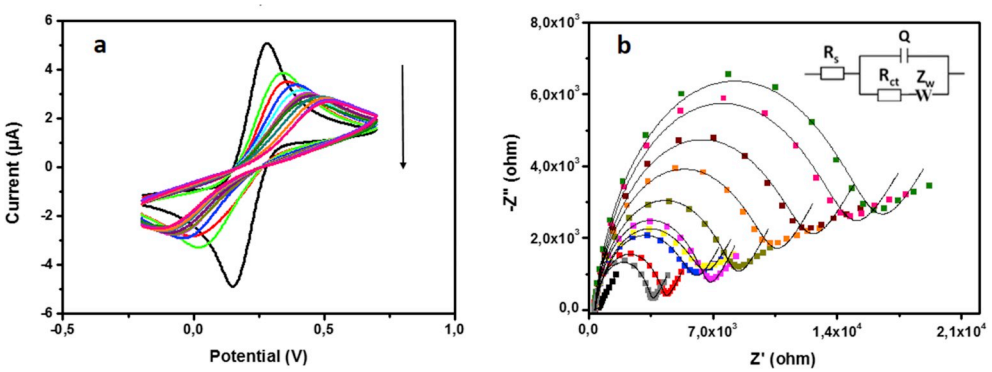

Fig. 4. (a) Cyclic voltammograms of the biosensor exposed to target genomic DNA: BGE (), MPTS, MPTS_AuNPs, MPTS_ AuNPs-DNA_{probe}, MPTS_ AuNPs-DNA_{probe}-BSA, MPTS_ AuNPs-DNA_{probe}-genome (0.6 pg μL^{-1}), Biosensor-genome (1.3 pg μL^{-1}), Biosensor-genome (2.6 pg mL^{-1}), Biosensor-genome (5.2 pg μL^{-1}), Biosensor-genome (10.4 pg μL^{-1}), Biosensor-genome (20.9 pg μL^{-1}), Biosensor-genome (40.0 pg μL^{-1}) and Biosensor-genome (83.9 pg μL^{-1}). **(b)** Nyquist plots of the biosensor after exposure to different concentrations of target genomic DNA and negative control: BGE (■), MPTS_AuNPs-DNA_{probe}-BSA ■, Biosensor-genome (0.6 pg μL^{-1}) ■, Biosensor-genome (1.3 pg μL^{-1}) ■, Biosensor-genome (2.6 pg μL^{-1}) ■, Biosensor-genome (5.2 pg μL^{-1}) ■, Biosensor-genome (10.4 pg μL^{-1}) ■, Biosensor-genome (20.9 pg μL^{-1}) (■, Biosensor-genome (40.0 pg μL^{-1}) ■, Biosensor-genome (83.9 pg μL^{-1}) ■ and Biosensor-negative control ■. The solid lines represent the simulation data. **Inset:** Randles equivalent circuit.

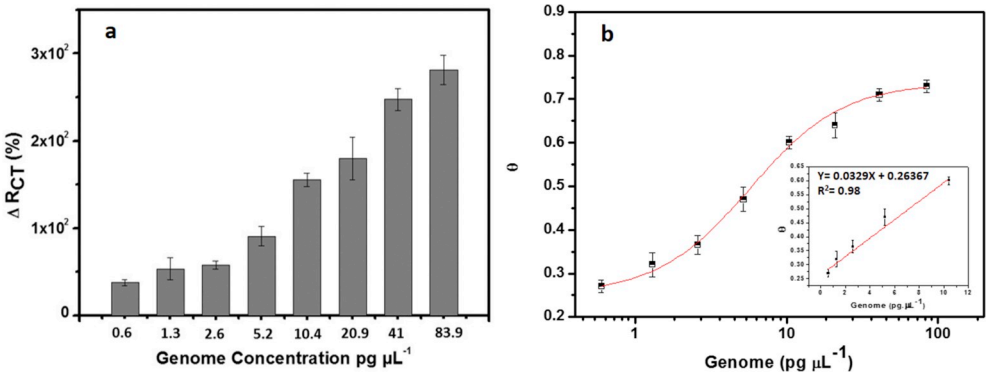

Fig. 5. (a) ΔRct% and **(b)** Θ as a function of different concentrations of the genomic target sequence.

Table 1
Equivalent circuit values obtained from fitted impedance results.

Modified electrode	Genomic target sequence ($pg.\mu L^{-1}$)	R_{CT}/kΩ	Q/µF	n
Bare gold electrode	–	0.16	6.66	0.51
MPTS-AuNPs_DNA probe	–	3.84	2.08	0.86
Sensor system-DNA target	0.6	5.37	3.06	0.83
	1.3	5.85	3.06	0.83
	2.6	6.18	1.08	0.86
	5.2	7.64	1.23	0.86
	10.4	9.59	1.74	0.86
	20.9	11.40	1.63	0.87
	41.0	13.70	1.51	0.88
	83.9	15.10	1.44	0.89
Negative control	–	4.06	0.94	0.91
Sensor system-urine sample	50.0	9.0	0.90	0.91
	40.0	7.18	0.99	0.89
	36.0	6.42	1.06	0.90
	30.0	5.37	0.98	0.90
	27.0	4.94	1.10	0.91
Sensor system-CSF sample	60.0	11.3	2.78	0.85
	47.0	8.57	2.93	0.79
	34.0	6.11	1.92	0.85
	30.0	5.39	2.04	0.83
	25.0	4.50	3.03	0.82
Sensor system-serum sample	42.0	7.58	0.65	0.92
	39.0	6.92	0.55	0.93
	35.0	6.27	0.60	0.93
	31.0	5.63	0.93	0.90
	27.0	4.91	1.10	0.90

neuroschistosomiasis. Table 1 shows the R_{CT}% values of the samples containing DNA from the adult worm of *S. mansoni*. PCR was used to validate the concentrations of the genomic DNA from *S. mansoni.* There was no significant difference in DNA concentration detection by both measurement methods. The obtained values were used to get a reference standard curve with a limit of detection (LOD) of 0.6 pg μL^{-1}.

Also, *S. mansoni* can be detected in other biological fluids, such as urine and serum. Urine is not a conventional sample for diagnosis of *S. mansoni* but is promisor for DNA research. Urine has the great advantage of not being a sample of invasive collection and being easily obtainable. In this study, CSF, urine, and serum samples were analyzed under the same parameters. A significant increase in the R_{CT} values was obtained after the recognition of positive samples.

The sensitivity of the genosensor was evaluated through a calibration curve obtained from impedimetric responses obtained after its exposure to the target sample. The biosensor has demonstrated excellent sensitivity for detecting the genomic target at low concentrations in CSF, urine, and serum. Table 1 shows the fitted impedance parameters for different samples. The proposed biosensor is effective at low sample volumes (2 µL). The comparison of the proposed genosensor with other previous biosensors is shown in Table 2. Thus, the present biosensor demonstrated the feasibility for rapid molecular detection of *S. mansoni* compared with other methods.

3.4. Selectivity and stability of the genosensor

The adsorption of interfering molecules on the electrode surface is a factor that can modify the electrochemical response [43] and suppress the electrode response [44]. The interferents tested in this work were ascorbic acid (AA) and cholesterol. Fig. S2 shows the impedimetric response of the genosensor in the presence of the complex mixtures (analyte + interfering substances). The results indicate that the response of the genosensor was not significantly affected in the presence of substances usually found in biological fluids such as AA and cholesterol.

The reusability of the biosensor was evaluated immerging the genosensor in a solution of 5 mM NaOH for 5 min to unbound the genome. This process was repeated two more times on the same day (Figs. S3a and S3b). After 48 h of storage under refrigeration, the analytical tests were carried out under the same experimental conditions (Figs. S3c and

Table 2
Comparison of the analytical performances of the proposed genosensor with other biosensors for the detection of *Schistosoma sp.*

Type of biosensor	Analyte	Detect technique	Linear range	Limit	Reference
Piezoelectric immunosensor	*S. japonicum*	quartz crystal	10–200 ng mL^{-1}	5 ng mL^{-1}	[45]
Screen-Printed Biosensor	*S. mansoni*	cyclic and differential pulse voltammetry	0.038–20 ng mL^{-1}	0.038 ng mL^{-1}	[46]
Electrochemical biosensor	*Schistosoma* egg antigen	anodic stripping voltammetry (ASV)	0.02–1 µg mL^{-1}	0.01 µg mL^{-1}	[47]
Electrochemical immunoassay	*S. japonicum*	stripping voltammetry	2 ng mL^{-1} - 15 µg mL^{-1}	1.3 ng mL^{-1}	[48]
Spectroelectrochemical immunoassay	Soluble Egg Antigen (SEA)	UV/Vis spectrometry and cyclic voltammetry	–	3.31 × 10^{-5} ng mL^{-1}	[49]
Electrochemical immunoassay	*S. japonicum*	linear sweep voltammetry (LSV)	1:5000–1:100	1:6457	[50]
Metalloimmunoassay	*S. japonicum* antibody	anodic stripping voltammetry (ASV)	6.4 ng mL^{-1} - 100 µg mL^{-1}	3.0 ng mL^{-1}	[51]
Genosensor	*S. mansoni*	Cyclic voltammetry and Impedance spectroscopy electrochemical	27–50 pg μL^{-1} (urine) 25–60 pg μL^{-1} (CSF) 27–42 pg μL^{-1} (serum)	6.0 ng mL^{-1}	This work

S3d). Thus, it was possible to confirm the stability of the genosensor. Therefore, the proposed sensor is a useful platform for rapid and specific detection of *S. mansoni* in different biological fluids as CSF, urine, and serum.

4. Conclusion

A novel electrochemical sensing platform based on a self-assembled layer of 3-mercaptopropyltrimethoxysilane and electrochemically synthesized AuNPs for diagnosis of schistosomiasis was successfully developed. The impedimetric and voltammetric analyses were effective to evaluate the process of modifying the electrode surface. The developed genosensor showed excellent performance in the detection of target genomic sequences at low concentrations in CSF, urine, and serum with a limit of detection (LOD) of 0.6 pg μL^{-1}. The developed system is presented as a promising alternative for the label-free detection of Schistosoma in CSF, urine, and serum.

Acknowledgments

G.S. Santos would like to thank CAPES for a Ph.D. scholarship. Oliveira and Andrade would like to thank National Council for Scientific and Technological Development - CNPq (grants 314894/2018-7 and 314756/2018-3).

Appendix A. Supplementary data

Supplementary data to this article can be found online at https://doi.org/10.1016/j.talanta.2019.05.111.

References

[1] K.G. Weerakoon, G.N. Gobert, P. Cai, D.P. McManus, Advances in the diagnosis of human schistosomiasis, Clin. Microbiol. Rev. 28 (4) (2015) 939–967.
[2] WHO, Schistosomiasis, Number of people treated worldwide in 2014, Wkly. Epidemiol. Rec. 5 (91) (2016) 53–60.
[3] R.G. Scholte, L. Gosoniu, J.B. Malone, F. Chammartin, J. Utzinger, P. Vounatsou, Predictive risk mapping of schistosomiasis in Brazil using Bayesian geostatistical models, Acta Trop. 132 (2014) 57–63.
[4] M.F. Rose, E.E. Zimmerman, L. Hsu, A.J. Golby, E. Saleh, R.D. Folkerth, S.S. Santagata, D.A. Milner Jr., S.H. Ramkissoon, Atypical presentation of cerebral schistosomiasis four years after exposure to Schistosoma mansoni, Epilepsy Behav Case Rep 2 (2014) 80–85.
[5] WHO, Schistosomiasis and soil-transmitted helminthiases: number of people treated in 2015, Wkly. Epidemiol. Rec. 91 (2016) 585–600.
[6] A.R. Prata, J.R. Coura, Fases e formas clínicas da Esquistossomose mansoni, in: O.S. Carvalho, P.M.Z. Coelho, H.L. Lenzi, orgs (Eds.), Schitosoma mansoni e esquistossomose: uma visão multidisciplinar [online], Fiocruz,Rio de Janeiro, 2008, pp. 739–787.
[7] M.J. Van Der Werf, S.J. De Vlas, Morbidity and infection with schistosomes and soil transmitted helminthes, Acta Trop. 86 (2001) 1–3.
[8] I.S. Bruscky, F.L. de Melo, Z.M. de Medeiros, F.F. Albuquerque, L.B. Wanderley, C. da Cunha-Correia, Nested polymerase chain reaction in cerebrospinal fluid for diagnosing spinal cord schistosomiasis: a promising method, J. Neurol. Sci. 366 (2016) 87–90.
[9] J.M. Yu, S.J. de Vlas, Q.W. Jiang, B. Gryseels, Comparison of the Kato-Katz technique, hatching test and indirect hemagglutination assay (IHA) for the diagnosis of Schistosoma japonicum infection in China. Parasitol. Int. 56 (2007) 45–49.
[10] D.D. Lin, J.X. Liu, Y.M. Liu, F. Hu, Y.Y. Zhang, et al., Routine Kato-Katz technique underestimates the prevalence of Schistosoma japonicum: a case study in an endemic area of the People's Republic of China, Parasitol. Int. 57 (2008) 281–286.
[11] R.R. Vitorino, F.P.C. Souza, A.P. Costa, F.C. Faria, L.S. Junior, A.P. Gomes, Schistosomiasis mansoni: diagnosis, treatment, epidemiology, prophylaxis and control, Rev. Bras. Ciência Mov. 10 (2012) 39–45.
[12] M. Booth, P. Vounatisou, E.K. N'Goran, M. Tanner, S. Gedamu, et al., He influence of sampling effort and the performance of the Kato-Katz technique in diagnosing Schistosoma mansoni and hookworm co-infections in rural Cote d'Ivoire, Parasitol. Int. 127 (2003) 525–531.
[13] A.S. Andrade Filho, A.C. Queiroz, M.G. Reis, R.M. Amaral, R.M. Brito, Neuroesquistossomose, Rev. Neuropsiq. 19 (2015) 165–209.
[14] E.J. Oliveira, H.Y. Kanamura, L.C.S. Diasil, L.C.B. Soares, D.M.C. Lima, R.M.C. Ciaravolho, IgM-ELISA for diagnosis of schistosomiasis mansoni in low endemic areas, Cad. Saúde Pública 19 (2003).
[15] Brasil. Saúde., Guia de vigilância epidemiológica e controle da mielorradiculopatia esquistossomótica, Ronaldo Santos do Amaral, Brasília, 2006, p. 32.
[16] G. Harter, H. Frickmann, S. Zenk, D. Wichmann, B. Ammann, P. Kern, B. Fleischer, E. Tannich, S. Poppert, Diagnosis of neuroschistosomiasis by antibody specificity index and semi-quantitative real-time PCR from cerebrospinal fluid and serum, J. Med. Microbiol. 63 (2014) 309–312.
[17] P. Kara, C. Cavusoglu, S. Cavdar, M. Ozsoz, Direct electrochemical genosensing for multiple point mutation detection of Mycobacterium tuberculosis during the development of rifampin resistance, Biosens. Bioelectron. 24 (6) (2009) 1796–1800.
[18] A.C.H. Castro, E.G. Franc, L.F. de Paula, M.M.C.N. Soares, L.R. Goulart, J.M. Madurro, A.G. Brito-Madurrosince, Preparation of genosensor for detection of specific DNA sequence of the hepatitis B virus is possible convert the hybridization into a measurable electric signal, Appl. Surf. Sci. 314 (2014) 273–279.
[19] V.K. Gupta, M.L. Yola, M.S. Qureshi, A.O. Solak, N. Atar, Z. Üstündağ, A novel impedimetric biosensor based on graphene oxide/gold nanoplatform for detection of DNA arrays, Sensor. Actuator. B Chem. 188 (2013) 1201–1211.
[20] X. Yu, Y. Jiao, Q. Chai, Applications of gold nanoparticles in biosensors, Nano LIFE 06 (02) (2016) 1642001–1642011.
[21] M.L. Yola, N. Atar, A novel voltammetric sensor based on gold nanoparticles involved in p-aminothiophenol functionalized multi-walled carbon nanotubes: application to the simultaneous determination of quercetin and rutin, Electrochim. Acta 119 (2014) 24–31.
[22] M.L. Yola, T. Eren, N. Atar, A sensitive molecular imprinted electrochemical sensor based on gold nanoparticles decorated graphene oxide: application to selective determination of tyrosine in milk, Sensor. Actuator. B Chem. 210 (2015) 149–157.
[23] R. Oliveira, F.L. Pissetti, A.M.S. Lucho, Fto Modified Electrodes by Direct Gold Electrodeposition: Production, Characterization and Electrochemical Sensor Aplication, Quím. Nova, 2016, pp. 146–155.
[24] M.L. Yola, N. Atar, Z. Üstündağ, A.O. Solak, A novel voltammetric sensor based on p-aminothiophenol functionalized graphene oxide/gold nanoparticles for determining quercetin in the presence of ascorbic acid, J. Electroanal. Chem. 698 (2013) 9–16.
[25] A. Bonanni, M. del Valle, Use of nanomaterials for impedimetric DNA sensors: a review, Anal. Chim. Acta 678 (1) (2010) 7–17.
[26] A. Ramanavicius, N. German, A. Ramanaviciene, Evaluation of electron transfer in electrochemical system based on immobilized gold nanoparticles and glucose oxidase, J. Electrochem. Soc. 164 (2017) G45–G49.
[27] M. Etesami, N. Mohamed, Catalytic application of gold nanoparticles electrodeposited by fast scan cyclic voltammetry to glycerol electrooxidation in alkaline electrolyte, Int. J. Electrochem. Sci. 6 (2011) 4676–4689.
[28] A. Guiseppi-Elie, L. Lingerfelt, Impedimetric detection of DNA hybridization: towards near-patient DNA diagnostics, Top. Curr. Chem. 260 (2005) 161–186.
[29] I. Piwoński, J. Grobelny, M. Cichomski, J. Rogowski, Investigation of 3-mercaptopropyltrimethoxysilane self-assembled monolayers on Au(111) surface, Appl. Surf. Sci. 242 (0169–4332) (2005) 147–153.
[30] M. Etesami, N. Mohamed, Catalytic application of gold nanoparticles electrodeposited by fast scan cyclic voltammetry to glycerol electrooxidation in alkaline electrolyte, Int. J. Electrochem Sci. 6 (2011) 4676–4689.
[31] M.A.L. Silva, Z. Medeiros, C.R.P. Soares, E.D. Silva, D.B. Miranda-Filho, F.L. Melo, A comparison of four DNA extraction protocols for the analysis of urine from patients with visceral leishmaniasis, Rev. Soc. Bras. Med. Trop. 47 (2) (2014) 193–197.
[32] F.G. Abath, F.L. Melo, R.P. Werkhauser, L. Montenegro, R. Montenegro, H.C. Schindler, Single-tube nested PCR using immobilized internal primers, Biotechniques 33 (6) (2002).
[33] R. Das, M.K. Sharma, V.K. Rao, B.B.K.,I. Garg, V. Venkatesh, S. Upadhyay, An electrochemical genosensor for Salmonella typhi on gold nanoparticles-mercaptosilane modified screen printed electrode, J. Biotechnol. (2014) 9–16.
[34] M.D.L. Oliveira, M.L. Nogueira, M.T.S. Correia, L.C.B.B. Coelho, C.A.S. Andrade, Detection of dengue virus serotypes on the surface of gold electrode based on Cratylia mollis lectin affinity, Sensor. Actuator. B Chem. 155 (2) (2011) 789–795.
[35] D. Necas, P. Klapetek, C. Anderson, Gwyddion (2008).
[36] H.Y. Park, M.J. Schadt, I. Wang, S. Lim, P.N. Njoki, S.H. Kim, M.Y. Jang, J. Luo, C.J. Zhong, Fabrication of magnetic core@shell Fe oxide@Au nanoparticles for interfacial bioactivity and bio-separation, Langmuir 23 (2007) 9050–9056.
[37] H. Yi, W. Xu, Y. Yuan, Y. Wu, Y. Chai, R. Yuan, A sensitive electrochemical aptasensor for thrombin detection based on exonuclease-catalyzed target recycling and enzyme-catalysis, Biosens. Bioelectron. 47 (2013) 368–372.
[38] G.S. Santos, C.A. Andrade, I.S. Bruscky, L.B. Wanderley, F.L. Melo, M.D. Oliveira, Impedimetric nanostructured genosensor for detection of schistosomiasis in cerebrospinal fluid and serum samples, J. Pharm. Biomed. Anal. 137 (2017) 163–169.
[40] D.M.N. Luna, K.Y.P.S. Avelino, M.T. Cordeiro, C.A.S. Andrade, M.D.L. Oliveira, Electrochemical immunosensor for dengue virus serotypes based on 4-mercaptobenzoic acid modified gold nanoparticles on self-assembled cysteine monolayers, Sensor. Actuator. B Chem. 220 (2015) 565–572.
[41] J.B.B. Randles, Kinetics of rapid electrode reactions, Discuss. Faraday Soc. 1 (1947) 11–19.
[42] E.J. Choi, D. Kim, K.S. Yun, A Study on the Electrical Circuit Model for Impedance-Based Microfluidic Sensor, International Conference on Nanotechnology and Biosensors, Singapore, 2011, pp. 85–89.
[43] F.R.F. Leite, W.d.J.R. Santos, L.T. Kubota, Selective determination of caffeic acid in wines with electrochemical sensor based on molecularly imprinted siloxanes, Sensor. Actuator. B Chem. 193 (2014) 238–246.
[44] D. Diamond, Principles of Chemical and Biological Sensors, John Wiley e sons. Inc., 1998.
[45] Z. Wu, J. Wu, S. Wang, G. Shen, R. Yu, An amplified mass piezoelectric immunosensor for Schistosoma japonicum, Biosens. Bioelecton. 22 (2006) 207–212.
[46] M. Shohayeb, H. Arida, G.A.M. Mersal, M. El-Badawy, Development of a nanotechnology - based printed biosensor for detection of Schistosoma mansoni antibodies, Int. J. Electrochem. Sci. 11 (2016) 1337–1344.

[47] L. Xu, J. Du, Y. Deng, N. He, Fabrication of magnetic porous pseudo-carbon paste electrode electrochemical biosensor and its application in detection of schistosoma egg antigen, Electrochem. Commun. 12 (2010) 1329–1332.
[48] J. Nie, Y. Zhang, W. Wang, Superhydrophobic surface-based magnetic electrochemical immunoassay for detection of Schistosoma japonicum antibodies, Biosens. Bioelectron. 33 (2010) 23–28.
[49] J. Odundo, N. Noah, D. Andala, J. Kiragu, M. Ndikau, G. Kimani, J. Mwatha, Spectro-electrochemical characterization of anti-schistosoma- gold nanoparticles conjugate for use in immunoassays, J. Korean Chem. Soc. 9 (2016) 35–45.
[50] X. Quing, X. Chu, G. Shen, R. Yu, Electrochemical detection of Schistosoma japonicum antibody using biocatalytic deposition, Anal. Lett. 41 (2008) 2237–2250.
[51] X. Chu, Z. Xiang, X. Fu, S. Wang, G. Shen, R. Yu, Silver-enhanced colloidal gold metalloimmunoassay for Schistosoma japonicum antibody detection, J. Immunol. Methods 301 (2005) 77–88.